IOP PUBLISHING JOURNAL OF PHYSICS: CONDENSED MATTER

J. Phys.: Condens. Matter **24** (2012) 024220 (8pp) doi:10.1088/0953-8984/24/2/024220

Determination of the spin torque non-adiabaticity in perpendicularly magnetized nanowires

J Heinen[1], D Hinzke[1], O Boulle[2], G Malinowski[3], H J M Swagten[4], B Koopmans[4], C Ulysse[5], G Faini[5], B Ocker[6], J Wrona[6] and M Kläui[1,7,8,9]

[1] Fachbereich Physik, Universität Konstanz, 78457 Konstanz, Germany
[2] Spintec, UMR CEA/CNRS/UJF-Grenoble 1/Grenoble-INP, 38054 Grenoble Cedex 9, France
[3] Laboratoire de Physique des Solides, Université Paris-sud, 91405 Orsay, France
[4] Department of Applied Physics, Eindhoven University of Technology, 5600 MB, The Netherlands
[5] CNRS, Phynano Team, Laboratoire de Photonique et de Nanostructures, 91460 Marcoussis, France
[6] Singulus Technologies AG, 63796 Kahl am Main, Germany
[7] SwissFEL, Paul Scherrer Institut, 5232 Villigen PSI, Switzerland
[8] Laboratory for Nanomagnetism and Spin Dynamics, Ecole Polytechnique Fédérale de Lausanne (EPFL), 1015 Lausanne, Switzerland
[9] Institut für Physik, Johannes Gutenberg-Universität, 55099 Mainz, Germany

E-mail: Mathias.Klaeui@magnetism.ch

Received 4 July 2011, in final form 20 October 2011
Published 15 December 2011
Online at stacks.iop.org/JPhysCM/24/024220

Abstract

Novel nanofabrication methods and the discovery of an efficient manipulation of local magnetization based on spin polarized currents has generated a tremendous interest in the field of spintronics. The search for materials allowing for fast domain wall dynamics requires fundamental research into the effects involved (Oersted fields, adiabatic and non-adiabatic spin torque, Joule heating) and possibilities for a quantitative comparison. Theoretical descriptions reveal a material and geometry dependence of the non-adiabaticity factor β, which governs the domain wall velocity. Here, we present two independent approaches for determining β: (i) measuring the dependence of the dwell times for which a domain wall stays in a metastable pinning state on the injected current and (ii) the current–field equivalence approach. The comparison of the deduced β values highlights the problems of using one-dimensional models to describe two-dimensional dynamics and allows us to ascertain the reliability, robustness and limits of the approaches used.

(Some figures may appear in colour only in the online journal)

1. Introduction

The probably best known data storage device is the magnetic hard disk [1], which during the past few years has started to face stiff competition from novel memory concepts [2–5]. Flash memory, MRAM and racetrack memory are based on the usage of electric currents and charges to store and control information. The latter two are based on magnetic materials and therefore potentially share the advantage of virtually unlimited endurance and good data retention with the magnetic hard disk. Furthermore, their advantages over hard drives are fast access times and the feature that they work without mechanically moving parts, which is energy-consuming.

Despite the new approaches used to manipulate the magnetization, the interpretation of information (bits 0 and 1) as magnetic domains pointing in a left/right (up/down) direction remains. So called domain walls (DWs) separate the domains from each other and the size of the domain and the DW width are thus limiting the data storage density. Various

effects can be used to manipulate magnetic domains and the DWs delineating them. In the case of magnetic disk drives, a read/write head is moved mechanically across a magnetic material and allows for a local manipulation of the domains using an external field. Nowadays, novel nanofabrication methods open a new path to encoding information within a simple nanowire structure on a scale of a few hundred nanometers. Here, localized injection of current is used to manipulate the magnetization using various effects. The most obvious effect is the creation of an Oersted field, which is commonly used to create DWs. The more exciting effect is the interaction of a spin polarized current with the local magnetization, especially the influence on the DW dynamics. This interaction is mainly characterized by two torques: (i) the adiabatic torque and (ii) the non-adiabatic torque, which is caused by several mechanisms. In experiments it was found that these effects are strongly dependent on the materials used and the magnetization configuration (in-plane or out-of-plane). Introducing the non-adiabaticity factor β, which governs the DW velocities, allows for the comparison between the experiments. Nevertheless, a wide variety of values has been found, highlighting the problems in separating the aforementioned effects and their quantitative description.

In this paper, we focus on approaches for determining the contribution of the Oersted field effect and spin torque to the current-induced domain wall dynamics. Two experimental approaches are presented, which we use to deduce the spin torque non-adiabaticity β, and we discuss their reliability considering the 2D nature of the DWs when using 1D models.

2. The theory of torques acting on domain walls

2.1. Field-induced domain wall motion (Oersted field effects)

The most obvious effect to manipulate magnetic domains is an externally applied magnetic field, which can drive a single domain wall, but will move two adjacent domain walls in opposite directions. In addition to causing the spin torque effects described below, a charge current which is flowing in a non-magnetic or magnetic material is also creating a local Oersted field according to the Biot–Savart law. This Oersted field can create and move a DW [6–10]. On the nanoscale, disadvantages of this approach arise, because high current densities are needed to create the necessary large magnetic fields and this entails disadvantageous scaling. However, in this work we focus just on currents flowing in a magnetic wire that also contains the domain walls and so we do not deal with the Oersted field created externally in separate structures. But a current flowing through a magnetic nanowire also creates an Oersted field. Simulations of a perfect nanowire show that the net force on a DW should be zero, but in out-of-plane magnetized materials it can lead to local depinning of the DW at the edges of the wire, where an effective local Oersted field is present. For soft-magnetic materials with a perpendicular uniaxial anisotropy it might also lead to a complete change of the domain structure, e.g. a change to DWs aligned along the wire, which then can be reversibly switched due to the Oersted field [11].

2.2. Adiabatic torque

Another approach for locally manipulating the magnetization within nanostructured devices was first introduced by Berger more than 30 years ago [12]. This approach is based on the interaction of spin polarized conduction electrons with the local magnetization. When crossing a sufficiently wide DW, the conduction electron spins can adiabatically follow the local magnetization, transferring angular momentum due to the conservation of total spin and thus driving a domain wall along the electron flow direction [13–15]. The wall velocity u resulting from this angular momentum transfer can be calculated as follows: $u = JPg\mu_B/2eM_S$, where μ_B is the Bohr magneton,

P is the current spin polarization and M_S is the saturation magnetization [13, 14].

2.3. Non-adiabatic torque

In the case of a narrow DW, non-adiabatic effects can occur, which were first introduced by Zhang *et al* [15] and Thiaville *et al* [16] in describing spin relaxation processes (SR) [14–17] and a linear momentum transfer (NA) [13, 14, 18–20]. These effects can significantly alter the DW dynamics as regards DW velocity and critical current density. Introducing a dimensionless non-adiabaticity factor $\beta = \beta_{SR} + \beta_{NA}$ including both non-adiabatic contributions, the final velocity now scales below the Walker breakdown as follows: $v = \frac{\beta}{\alpha}u$ where α is the Gilbert damping constant [15, 17, 21]. Therefore, the search for materials with a large non-adiabaticity factor β is a focus of spintronic research.

2.4. Description using a 1D model with and without thermal excitation

Using a set of two parameters (DW center position q, effective out-of-plane angle Ψ) it is possible to describe the DW dynamics for a rigid domain wall profile [16]:

$$\dot{\Psi} + \frac{\alpha\dot{q}}{\lambda} = \gamma\mu_0 H + \frac{\beta u}{\lambda} - \frac{\gamma}{2M_S}\frac{\delta V_{pin}}{\delta q} \quad (1)$$

$$\frac{\dot{q}}{\lambda} - \alpha\dot{\Psi} = \frac{\gamma\mu_0 H_k}{2}\sin 2\Psi + \frac{u}{\lambda} \quad (2)$$

where $\gamma = g\mu_B/\hbar$ is the gyromagnetic ratio, H_k is the restoring field for the transverse orientation, H is the applied perpendicular external magnetic field, $u = JPg\mu_B/2eM_S$ is the DW velocity and $V_{pin}(q, \Psi)$ is the pinning potential. The domain wall width is defined as $\lambda = \sqrt{\frac{A_{ex}}{K_0 + K\sin^2\Psi}}$ where A_{ex} is the exchange constant, K_0 is the uniaxial longitudinal anisotropy and K is the transverse anisotropy [22]. In the pure adiabatic case ($\beta = 0$) a critical current density J_c is necessary to drive a DW with the velocity $u_c = \gamma\mu_0 H_k\lambda/2$, which is derived by finding the stationary solutions of equations (1) and (2) [17, 21].

In most experiments the critical current density exceeds 1×10^{12} A m^{-2} leading to significant Joule heating effects, which are not taken into account so far in this 0 K model.

The 1D model described above can be extended by adding stochastic Gaussian distributed forces η_Ψ and η_q to account for thermal effects. This approach was introduced by Duine *et al* [23]. Following his approach, one can rewrite the equations of motion as

$$\dot{\Psi} + \frac{\alpha \dot{q}}{\lambda} = -\frac{\gamma}{2M_S}\frac{\delta V_{\text{eff}}}{\delta q} + \eta_\Psi \tag{3}$$

$$\frac{\dot{q}}{\lambda} - \alpha\dot{\Psi} = -\frac{\gamma}{2M_S\lambda}\frac{\delta V_{\text{eff}}}{\delta \Psi} + \eta_q \tag{4}$$

including an effective potential, which summarizes the terms for the adiabatic and non-adiabatic torques, the external field H, the demagnetizing field H_K and the pinning potential $V_{\text{pin}}(q, \Psi)$:

$$V_{\text{eff}} = \mu_0 H_K M_S \lambda \sin^2\Psi + \frac{2M_S}{\gamma}u\Psi - 2M_S q\left(\mu_0 H + \frac{\beta u}{\lambda\gamma}\right) + V_{\text{pin}}(q, \Psi). \tag{5}$$

Associated with V_{eff} one can now calculate the energy barrier ϵ, which a DW has to overcome.

2.5. Extracting the non-adiabatic spin torque (β)

One of the key challenges in the field of current-induced domain wall motion is to determine to what extent the adiabatic torque, the non-adiabatic torque and the Oersted field contribute to the wall displacement. The most important question is to understand the spin torque effect including the efficiency of the non-adiabatic torque and thus the value of β. Two independent approaches for extracting the non-adiabaticity have been put forward: (i) using the current–field equivalence and (ii) measuring the influence of current on the motion of a domain wall across an energy barrier, which a DW has to overcome before DW displacement occurs.

2.5.1. Current–field equivalence. The first approach can directly be deduced from the equations of motion of the 1D model. From equations (1) and (2) it can be seen that the non-adiabatic torque enters as an effective field $\mu_0 H_{\text{eff}} = \beta u/\gamma\lambda = \epsilon J$ with the efficiency $\epsilon = \beta P\hbar\pi/(2eM_S\lambda)$ [24, 25]. The efficiency can now be determined by studying the interaction of applied fields and injected currents, e.g. during DW depinning processes. This current–field equivalence is also independent of the concrete spin structure.

2.5.2. The Arrhenius law approach. The second approach is based on the assumption that a rigid and simple DW can be described as a quasiparticle moving in a 1D potential landscape. Here, we consider the case of a DW hopping between two metastable states, where the thermally activated motion from one energy potential well to another can be described by the Arrhenius law [26]. The dwell time τ_S for which a DW stays in one state S is an exponential function of the current dependent energy barrier $\epsilon(J)$ [26, 27]:

$$\frac{1}{\tau_S} = \frac{1}{\tau_{0,S}}e^{-\frac{\epsilon(J)}{k_B T}} \tag{6}$$

and therefore a strong influence from even small current densities J is expected. For the current dependent shift in energy, Eltschka *et al* [28] derived the following expression:

$$\epsilon_J = \frac{2\beta A\hbar P}{e}\frac{X_0}{\lambda}J \tag{7}$$

where e is the electron charge, A is the DW cross-sectional area, P is the spin polarization, X_0 is the hopping distance and λ is the domain wall width. Having determined the dwell times for which a domain remains in a state, one can use the following equation:

$$\ln\left(\frac{\tau_1}{\tau_0}\right) = \ln\left(\frac{\tau_{0,1}}{\tau_{0,0}}\right) + \frac{\epsilon_{0,1} - \epsilon_{0,0}}{k_B T} + \sigma J \tag{8}$$

where $\sigma = \frac{2A\hbar\beta P X_0}{k_B T e\lambda}$ is used to calculate the non-adiabaticity β.

2.6. Joule heating effects

Another effect which occurs when injecting high current densities into nanowires is Joule heating. This effect may lead to local temperature increases up to a few hundred kelvins [24, 29] depending on the wire structure, the material composition and the possibility of heat dissipation [30, 31] into the surrounding environment, and therefore alters the experimental settings. For example, in depinning field experiments, thermal energy helps the DW to overcome the pinning barrier and thus affects the necessary torque, which is the focus of most studies.

3. Experiments

To tailor materials that exhibit fast domain wall motion resulting from large non-adiabatic effects, one wants to enhance the non-adiabaticity and this is expected to occur for strong magnetization gradients, which are present in out-of-plane magnetized materials. These materials are characterized by a strong uniaxial anisotropy pointing out of the film plane, which is defined as $K_{\text{eff}} = K - \mu_0 M_S^2/2$ with the transverse anisotropy K and the shape anisotropy. In out-of-plane magnetized nanowires two domain wall types are possible [22, 32, 33]: (i) the Bloch walls, where the current is always flowing perpendicular to the local magnetization, and (ii) the Néel type walls, which are stable in the case of e.g. Co/Ni nanowires with widths below 100 nm [9]. Both DW types and their dynamics can be described as a first approximation using the 1D model. The theoretical approaches described above are also suitable for describing the experimental results and especially for extracting the spin torque non-adiabaticity. Therefore, nanowires with a strong perpendicular anisotropy using a Pt(2 nm)/[Co(0.6 nm)/Pt(1.4 nm)]$_2$/Co(0.6 nm)/Pt(2 nm) multilayer material and attached Hall crosses have been fabricated on an Si/SiO$_2$(220 nm) substrate by sputtering (see figure 1(a)). The effective easy-axis magnetic anisotropy $K_{\text{eff}} = 2.7 \times 10^5$ J m^{-3} (at 300 K) and the saturation magnetization $M_S = 1.4 \times 10^6$ A m^{-1} were determined previously [24]. Assuming an exchange constant $A_{\text{ex}} = 1.6 \times 10^{-11}$ J m^{-1} [34] allows us to estimate the DW width

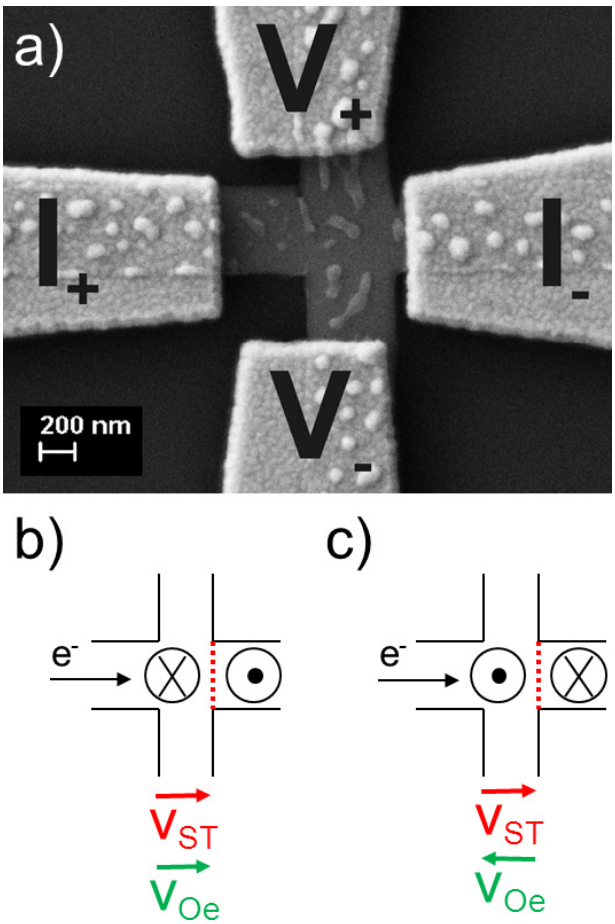

Figure 1. (a) Scanning electron microscopy image of the Hall cross geometry [Pt(2 nm)/[Co(0.6 nm)/Pt(1.4 nm)]$_2$/Co(0.6 nm)/Pt(2 nm)] used to detect and pin DWs. The current (I) and voltage (V) contacts are indicated. Remaining resist from the lift-off process can be seen. Injection of current along the wire leads to the creation of a concentric Oersted field and a spin torque. The spin torque will move the DW with a velocity (V_{ST}) to the right independent of the magnetization configuration along the electron flow direction. In contrast, the created Oersted field will move the DW in the same direction as the current in case (b), whilst it will move it in the opposite direction in case (c) indicated by DW velocities (V_{Oe}) of opposite direction. Adapted from [36].

$\lambda = \sqrt{\frac{A_{ex}}{K_{eff}}} \approx 6.3$ nm in our wires, which is much smaller than those in in-plane magnetized materials with comparable wire geometries [28, 35].

Nanowire structures using Cu(6 nm)/[Ni(0.6 nm)/Co(0.2 nm)]$_5$ as a multilayer material are fabricated as well. Extraordinary Hall measurements using an external field perpendicular to the wire plane reveal square hysteresis loops. The material parameters of similar Co/Ni multilayer materials have been measured by several groups [7, 9, 29]: saturation magnetization $M_S \approx 6.6 \times 10^5$ A m^{-1} and $K_{eff} \approx 4.1 \times 10^5$ J m^{-3}. Assuming again an exchange constant $A_{ex} = 1.6 \times 10^{-11}$ J m^{-1} one finds a DW width $\lambda \approx 6.2$ nm.

3.1. Separating the torques acting

For all of the effects described, one can find the following symmetries considering the configuration of the local magnetization and the polarity of the injected current:

(1) The Joule heating effect: this effect is independent of the magnetization configuration and the polarity of the injected current, leading in most cases to a reduction of a pinning potential, and therefore reduces the necessary depinning field of a DW with increasing current and thus heating.

(2) The Oersted field effect: depending on both parameters, polarization of current and local magnetization, this effect will be inverse when the current polarity (I_+ or I_-) or the magnetization in the domain (M_+ or M_-) is reversed (see figures 1(b) and (c)): $H_{Oe}(I_+, M_+) = -H_{Oe}(I_+, M_-)$ and $H_{Oe}(I_+, M_+) = -H_{Oe}(I_-, M_+)$.

(3) The spin torque: the adiabatic and non-adiabatic contributions only depend on the current polarity and are independent of the initial magnetization configuration. This can be expressed as (see figures 1(b) and (c)) $H_{ST}(I_-, M_+) = H_{ST}(I_-, M_-) = -H_{ST}(I_+, M_+) = -H_{ST}(I_+, M_-)$.

The depinning field under the influence of current can therefore be expressed as follows: $H_{dep} = H_{ST} + H_{Oe} + H_{Joule}$ [36].

3.2. Experimental results: domain wall depinning in Co/Pt multilayer wires

Various experiments focus only on a single magnetization configuration in order to study the influence of current on the depinning field of a DW. In view of this, most of the experiments have not been able to clearly separate the contributions of each of the torques unambiguously. In the case of the out-of-plane materials, recent measurements revealed large β values (larger than α and even larger than for permalloy) [13, 24, 28, 29, 37–43]. This approach is valid, as we can show that a weak pinning regime Ib as defined in [17], where β governs the depinning, is present. A weak pinning regime Ia, where the adiabatic torque (the so called spin transfer in [17]) matters, can by excluded since the critical current density $j_c^{Ia)}$ is much larger than the maximum current density used in our experiments. Furthermore, we can exclude the intermediate pinning regime since no constant threshold current density for DW motion, which is predicted in [17], is present in the results shown below. Last, we exclude the strong pinning regime, where no DW motion would occur. An example for the strong pinning regime is presented by Bisig *et al* studying tunable steady-state DW oscillators [44].

Taking into account the symmetries of all the aforementioned effects and resulting torques, we have studied the variation of the depinning field as a function of injected current density in order to separate the contributions and extract the spin torque non-adiabaticity [36]. We first reproducibly place a DW at the entrance of a Hall cross with both possible initial magnetization configurations (see figure 2(a)). We then start at zero field, where the extraordinary Hall voltage indicates that the DW is being reproducibly pinned at the same position. Performing the experiment at a low cryostat temperature reduces the possibility of a thermally activated DW depinning process. We observe a decrease of the depinning field with increasing current density and an obvious splitting between

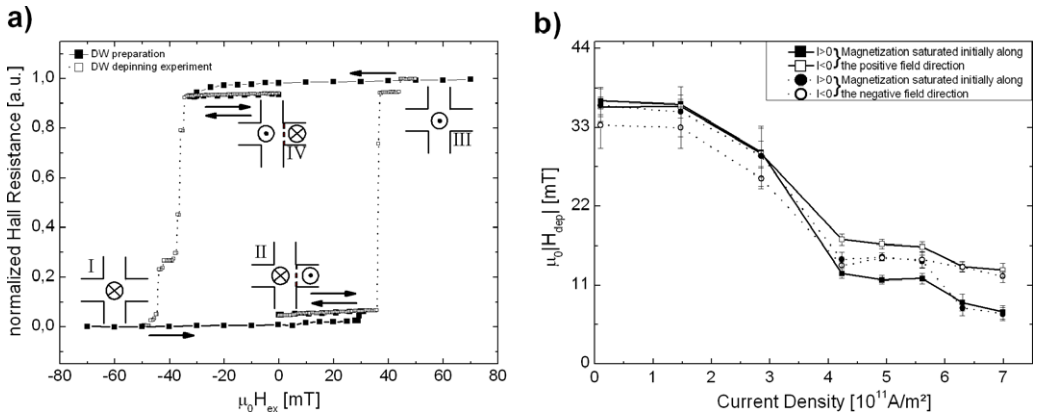

Figure 2. (a) Normalized Hall resistance as a function of the applied perpendicular external field at a constant cryostat temperature $T_{\mathrm{Cryo}} = 100$ K. The filled square, solid line curves correspond to the preparation of the DWs, while each point of the open square, dotted line curves is measured after the injection of a single pulse with a current density of $J = 1.02 \times 10^{10}$ A m^{-2}. (b) $|H_{\mathrm{dep}}|$ as a function of the injected current density for both initial magnetization configurations. The measurement points represent the mean values of $|H_{\mathrm{dep}}|$ averaged over at least eight repetitions, whilst the error bars show the standard deviation. Reproduced with permission from [36]. Copyright 2010 American Institute of Physics.

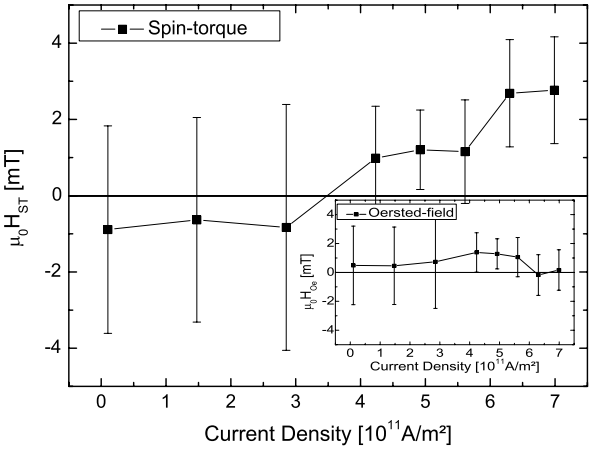

Figure 3. From the deduced contributions for spin torque and for the Oersted field (inset), we can extract the efficiency ϵ using a linear fit through the origin (zero spin torque for zero current density) and including the points with the lowest Oersted field contribution. Reproduced with permission from [36]. Copyright 2010 American Institute of Physics.

the two current polarities under the influence of injected current pulses (see figure 2(b)). The overall decrease can be attributed to Joule heating, whilst the splitting can be either due to Oersted field effects or spin torque effects. The combination of four measurements $(I_{\pm}, M_{\pm})$ allows us to deduce each contribution to the depinning field using the aforementioned symmetries (for details see [36]). The result shows almost zero Oersted field contribution and a non-zero spin torque contribution (see figure 3). As regards the adiabatic torque, the calculated critical current density J_{c} is much higher than the injected current densities used in the experiment and therefore does not contribute to the DW depinning.

3.2.1. Current–field equivalence. A quantitative description of the spin torque is given by the non-adiabaticity factor. Here, we used the current–field equivalence mentioned above. Analyzing the efficiency $\epsilon = \beta P\hbar\pi/(2eM_{\mathrm{S}}\lambda)$, which is defined as the slope $|\mu_0 \Delta H_{\mathrm{dep}}/\Delta J|$, allows us to directly deduce the non-adiabaticity factor β. The material parameters used are: current spin polarization $P = 0.46$ (assumed to be similar to that of pure Co), domain wall width $\lambda = 6.3$ nm and saturation magnetization $M_{\mathrm{S}} = 1.4 \times 10^6$ A m^{-1}. The Joule heating has been extracted during the calculations, but one has to consider that the sample temperature was changing during the pulse injection. Complementary experiments of Boulle *et al* [24] allow us to approximate the sample temperature increase during the pulse injection. We find that the sample temperature increases for the highest injected current densities up to 300 K, when starting at a constant cryostat temperature of 100 K, thus allowing us to compare the derived β values. It turns out that the derived $\beta = 0.24$ is of the same order of magnitude as compared to the derived value $\beta = 0.35$ obtained by Boulle *et al* [24] at a constant sample temperature (300 K) and almost double the Gilbert damping constant $\alpha \approx 0.15$ [45].

3.3. Experimental results: the dominant adiabatic spin torque in Co/Ni multilayer wires

The knowledge gained from the Co/Pt experiment (see section 3.2) allows us to extend these experiments to the Co/Ni multilayer material. Using a short wire structure (<2 μm) with attached Hall crosses, which are in close proximity to each other, we are able to inject short 10 ns long pulses to reduce Joule heating effects. Following the depinning field measurement scheme used before on the Co/Pt multilayer wires [36], we are able to separate the spin torque and Oersted field contribution at a constant cryostat temperature of 200 K. Since the material parameters are similar to the Co/Pt multilayer material ones and high DW velocities have been observed [46], one might expect to measure also high β values. The results from the depinning field measurements are shown in figure 4.

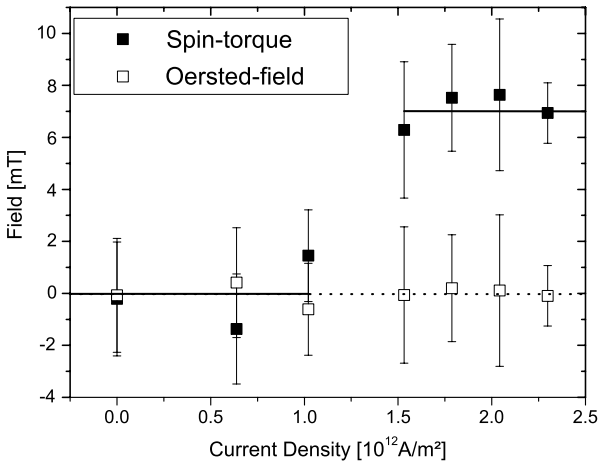

Figure 4. The spin torque and Oersted field contribution are deduced by following the measurement scheme used for the Co/Pt multilayers [36]. At a current density of 1.5×10^{12} A m^{-2} a step in the spin torque field is present.

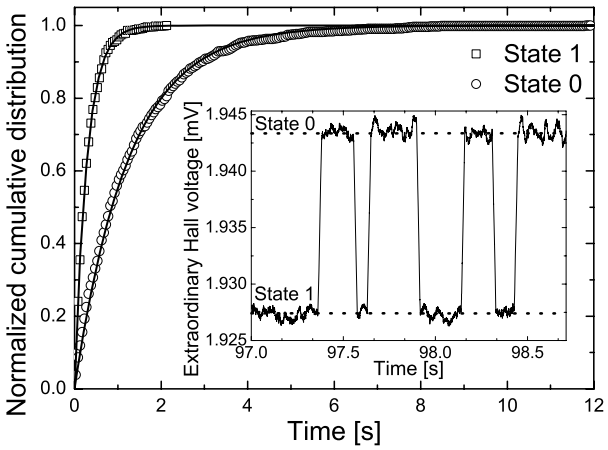

Figure 5. The normalized cumulative distribution for both metastable states is fitted using the cumulative distribution function $F(t) = 1 - e^{-\frac{t}{\tau_S}}$ to extract the dwell time τ_S of state S (solid lines). The inset shows the time-resolved extraordinary Hall voltage, revealing two metastable states for a constant field (3.41 Oe) and a constant current $|I| = 0.5$ mA, which corresponds to a current density of $J = 1.16 \times 10^{11}$ A m^{-2}. Reproduced with permission from [49]. Copyright 2011 American Institute of Physics.

The Oersted field contribution is zero within the error bars, whilst a non-zero contribution from spin torque effects exists at high current densities ($>1 \times 10^{12}$ A m^{-2}). In contrast to the case for the spin torque contribution of the Co/Pt measurements, here a step-like dependence is observed with a threshold current density of about 1.5×10^{12} A m^{-2}. This threshold current density and the fact that there is no linear dependence of the spin torque generated effective field on the current density point to the adiabatic torque as the driving mechanism and to $\beta \approx 0$. Measurements performed and published by other groups [7, 9] reveal a similar behavior, which is also explained by a dominant adiabatic spin torque requiring a critical current density to move the DW. The observed critical current density is of the same order of magnitude as in our present measurement.

3.4. Experimental results: thermally activated domain wall motion in Co/Pt multilayer wires

To further investigate the non-adiabaticity factor β at 300 K, we now study the thermally activated DW motion under the influence of external fields and small injected DC currents, which cause no significant Joule heating effects. The low current densities ($<1.2 \times 10^{11}$ A m^{-2}) used are also expected to be too small to significantly affect the shape of the DW. Using similar Co/Pt Hall cross structures we are able to measure the extraordinary Hall voltage in a time-resolved manner and to detect two metastable states (see figure 5 (inset)). Thermal activation keeps the DW moving back and forth between the two states. As theoretically predicted, we observe a strong influence of the applied DC current or the applied field on the dwell times for which the DW remains in the states. We record the signal for several minutes before changing the current and/or applied field to obtain sufficient statistics for the dwell times. The error of each dwell time is hereby defined as the standard deviation of the mean value. For the case of constant currents (constant fields), we can see that $\ln(\tau_1/\tau_0)$ scales linearly with the applied fields (applied DC currents).

3.4.1. Current–field equivalence. Figure 6(a) shows $\ln(\frac{\tau_1}{\tau_0})$ as a function of the applied field. It is shown that the reversal of the current polarity results in a translation of the values by a magnetic field ΔH using a fitted constant slope. This suggests that the injected current acts as an effective magnetic field. Again, we can use the current–field equivalence approach (using $\epsilon = |\frac{\Delta H}{\Delta J}| = \frac{\beta P \hbar}{2eM_S\lambda}$) to deduce β. For the various combinations of ΔH and ΔJ and considering their errors as weighing factors, we obtain an average value $\beta_{\text{effective}} = 0.13 \pm 0.02$. Repeating the experiment at a slightly lower temperature ($T \approx 287$ K) and using different metastable pinning states, we obtain β values ranging between 0.13 and 0.23 in line with the values obtained from the current–field equivalence in depinning field measurements mentioned in section 3.2.1.

3.4.2. The Arrhenius law approach. Next, we analyze the hopping measurements at constant fields. In figure 6(b), $\ln(\frac{\tau_1}{\tau_0})$ is plotted as a function of the applied DC current: here, we obtain values for β by following the Arrhenius approach. In order to do so, we analyze the current dependent shift in energy and use equation (8) to derive $\beta_{\text{Arrhenius}}$. The critical parameters—the DW cross-sectional area $A = 4300$ nm^2 and the hopping distance $X_0 = 14.5$ nm—can be approximated using the total change in extraordinary Hall voltage and the known width and thickness of the wire. From the measurements at different constant fields, average values $\beta_{\text{Arrhenius}} = 0.013 \pm 0.001$ at $T \approx 296.6$ K and $\beta = 0.028$ at $T \approx 287.2$ K can be extracted, which turn out to be one order of magnitude smaller than $\beta_{\text{effective}}$.

4. Conclusions

In conclusion, we study Co/Pt and Co/Ni multilayer materials with a strong perpendicular uniaxial anisotropy in order

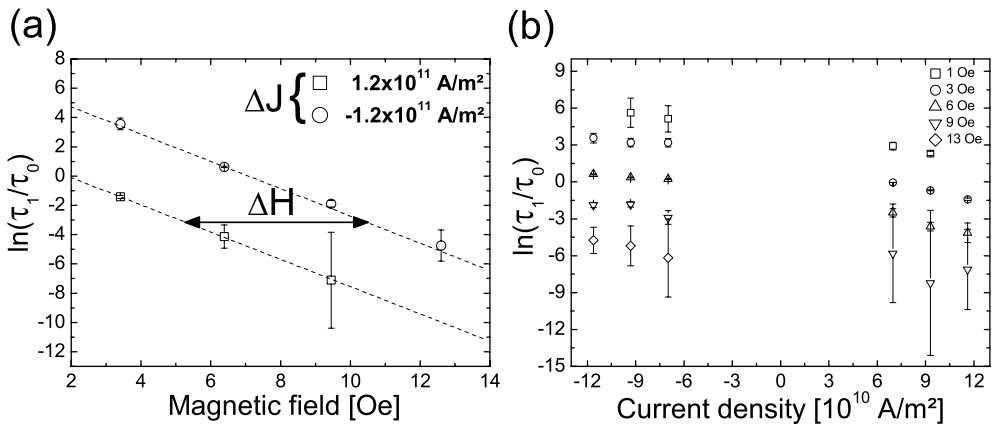

Figure 6. (a) $\ln(\frac{\tau_1}{\tau_0})$ as a function of the applied field for constant currents. For each value of a current we determine the slope by means of a linear fit weighed with errors of the individual measurements. The values of a current are then refitted using their average slope. (b) $\ln(\frac{\tau_1}{\tau_0})$ as a function of the injected current density for different constant fields. The non-adiabaticity factor β is calculated from the average slope of all fits. Reproduced with permission from [49]. Copyright 2011 American Institute of Physics.

to analyze the spin torque non-adiabaticity. Experimentally it is shown that we are able to separate the contributions to the DW depinning field and show that the Oersted field effect is negligibly small compared to the spin torque effects. We are also able to rule out the Joule heating effect causing a sample temperature increase. Nevertheless, for different Co/Pt sample structures we find consistent β values by following the current–field equivalence approach, thus showing that the high spin torque efficiency is intrinsic to the material and is not stemming from other spurious effects. In the case of the Co/Ni multilayer material, we extract a spin torque contribution, which is consistent with the adiabatic spin torque. An existing non-adiabatic spin torque contribution would have to be much smaller, as shown in our measurements. A discrepancy arises during the study of thermally activated DW motion on Co/Pt multilayer structures when analyzing the data from thermally activated DW motion experiments by using the Arrhenius law approach, which reveals a β value that is an order of magnitude smaller than the one deduced by the current–field approach. The parameters entered—cross-sectional area A and hopping distance X_0—that are necessary for solving equation (8) are calculated assuming a rigid and straight DW structure. This assumption necessary for a definition of X_0 and A might not hold for a DW entering a Hall cross with pinning sites. Deformations of a DW have previously been observed and a change of dimensionality has been shown by Kim *et al* [47]. Magnetic imaging techniques revealed here a transition from 1D to 2D behavior in the scaling criticality of creep DW motion as a function of the wire width. Related to the hopping distance, the activation volume is shown to no longer be proportional to the wire width in the 2D regime. A more accurate determination can in our case be achieved by examining the hopping distance via time-resolved magnetic imaging to measure X_0 and A. To compare to theory, full micromagnetic simulations at finite temperatures similar to those of Garcia-Sanchez *et al* [48] are necessary, where it is shown that the effective deduced activation volume can be smaller than that assumed from the hopping distance in the 1D model. Therefore, a large uncertainty of the displacement distance X_0 and cross-sectional area A might be present in our experiment, highlighting the problems when analyzing 2D dynamics with 1D models, while the current–field equivalence approach might prove more robust as it does not rely on these details.

Acknowledgments

The authors would like to acknowledge the financial support by the DFG (SFB 767, KL1811), the Landesstiftung Baden Württemberg, the European Research Council via its Starting Independent Researcher Grant (Grant No. ERC-2007-Stg 208162) scheme, EU RTN SPINSWITCH (MRTN-CT-2006035327), the EU STREP project MAGWIRE (FP7-ICT-2009-5 257707), the Swiss National Science Foundation and the Samsung Advanced Institute of Technology.

References

[1] McFadyen I, Fullerton E and Carey M 2006 *MRS Bull.* **31** 379
[2] Parkin S S P, Hayashi M and Thomas L 2008 *Science* **320** 190
[3] Cowburn R, Petit D, Read D and Petracic O 2007 *Patent WO* 2007/132174a1
[4] Xu P, Xia K, Gu C, Tang L, Yang H and Li J 2008 *Nature Nanotechnol.* **3** 97
[5] Pavan P, Bez R, Olivo P and Zanoni B 1997 *Proc. IEEE* **85** 1248
[6] Ilgaz D, Kläui M, Heyne L, Boulle O, Zinser F, Krzyk S, Fonin M, Rüdiger U, Backes D and Heyderman L J 2008 *Appl. Phys. Lett.* **93** 132503
[7] Ueda K *et al* 2011 *J. Phys.: Conf. Ser.* **266** 012110
[8] Koyama T, Yamada G, Tanigawa H, Kasai S, Ohshima N, Fukami S, Ishiwata N, Nakatani Y and Ono T 2008 *Appl. Phys. Express* **1** 101303
[9] Koyama T *et al* 2011 *Nature Mater.* **10** 194
[10] Tanigawa H *et al* 2009 *Appl. Phys. Express* **2** 053002
[11] Boulle O *et al* 2009 *J. Appl. Phys.* **105** 07C106
[12] Berger L 1978 *J. Appl. Phys.* **49** 2156
[13] Xiao J, Zangwill A and Stiles M D 2006 *Phys. Rev.* B **73** 054428
[14] Tatara G and Kohno H 2004 *Phys. Rev. Lett.* **92** 086601
[15] Zhang S and Li Z 2004 *Phys. Rev. Lett.* **93** 127204

[16] Thiaville A, Nakatani Y, Miltat J and Suzuki Y 2005 *Europhys. Lett.* **69** 990
[17] Tatara G, Takayama T, Kohno H, Shibata J, Nakatani Y and Fukuyama H 2006 *J. Phys. Soc. Japan* **75** 064708
[18] Vanhaverbeke A and Viret M 2007 *Phys. Rev.* B **75** 024411
[19] Waintal X and Viret M 2004 *Europhys. Lett.* **65** 427
[20] Tatara G, Kohno H and Shibata J 2008 *J. Phys. Soc. Japan* **77** 031003
[21] Thiaville A 2004 *J. Appl. Phys.* **95** 7049
[22] Porter D G 2004 *J. Appl. Phys.* **95** 6729
[23] Duine R A, Núñez A S and MacDonald A H 2007 *Phys. Rev. Lett.* **98** 056605
[24] Boulle O, Kimling J, Warnicke P, Kläui M, Rüdiger U, Malinowski G, Swagten H J M, Koopmans B, Ulysse C and Faini G 2008 *Phys. Rev. Lett.* **101** 216601
[25] Viret M, Vanhaverbeke A, Ott F and Jacquinot J-F 2005 *Phys. Rev.* B **72** 140403
[26] Hänggi P, Talkner P and Borkovec M 1990 *Rev. Mod. Phys.* **62** 251
[27] Attané J P, Ravelosona D, Marty A, Samson Y and Chappert C 2006 *Phys. Rev. Lett.* **96** 147204
[28] Eltschka M *et al* 2010 *Phys. Rev. Lett.* **105** 056601
[29] Burrowes C *et al* 2010 *Nature Phys.* **6** 17
[30] You C-Y, Sung I M and Joe B-K 2006 *Appl. Phys. Lett.* **89** 222513
[31] You C-Y and Ha S-S 2007 *Appl. Phys. Lett.* **91** 022507
[32] Jung S, Kim W, Lee T, Lee K and Lee H 2008 *Appl. Phys. Lett.* **92** 202508
[33] Mougin A, Cormier M, Adam J P, Metaxas P J and Ferré J 2007 *Europhys. Lett.* **78** 57007
[34] Metaxas P J, Jamet J P, Mougin A, Cormier M, Ferré J, Baltz V, Rodmacq B, Dieny B and Stamps R L 2007 *Phys. Rev. Lett.* **99** 217208
[35] Backes D *et al* 2007 *Appl. Phys. Lett.* **91** 112502
[36] Heinen J, Boulle O, Rousseau K, Malinowski G, Kläui M, Swagten H J M, Koopmans B, Ulysse C and Faini G 2010 *Appl. Phys. Lett.* **96** 202510
[37] Ravelosona D, Mangin S, Katine J A, Fullerton E E and Terris B D 2007 *Appl. Phys. Lett.* **90** 072508
[38] Fukami S, Suzuki T, Ohshima N, Nagahara K and Ishiwata N 2008 *J. Appl. Phys.* **103** 07E718
[39] Meier G, Bolte M, Eiselt R, Krüger B, Kim D and Fischer P 2007 *Phys. Rev. Lett.* **98** 187202
[40] Thomas L, Hayashi M, Jiang X, Moriya R, Rettner C and Parkin S S P 2006 *Nature Phys.* **443** 197
[41] Miron I M, Zermatten P-J, Gaudin G, Auffret S, Rodmacq B and Schuhl A 2009 *Phys. Rev. Lett.* **102** 137202
[42] San Emeterio Alvarez L, Wang K-Y, Lepadatu S, Landi S, Bending S J and Marrows C H 2010 *Phys. Rev. Lett.* **104** 137205
[43] Heyne L *et al* 2010 *Phys. Rev. Lett.* **105** 187203
[44] Bisig A, Heyne L, Boulle O and Kläui M 2009 *Appl. Phys. Lett.* **95** 162504
[45] Barman A, Wang S, Hellwig O, Berger A, Fullerton E E and Schmidt H 2007 *J. Appl. Phys.* **101** 09D102
[46] Koyama T, Chiba D, Ueda K, Tanigawa H, Fukami S, Suzuki T, Ohshima N, Ishiwata N, Nakatani Y and Ono T 2011 *Appl. Phys. Lett.* **98** 192509
[47] Kim K-J, Lee J-C, Ahn S-M, Lee K-S, Lee C-W, Cho Y J, Seo S, Shin K-H, Choe S-B and Lee H-W 2009 *Nature* **458** 740
[48] Garcia-Sanchez F, Szambolics H, Mihai A P, Vila L, Marty A, Attané J-P, Toussaint J-C and Buda-Prejbeanu L D 2010 *Phys. Rev.* B **81** 134408
[49] Heinen J, Hinzke D, Boulle O, Malinowski G, Swagten H, Koopmans B, Ulysse C, Faini G and Klaui M 2011 *Appl. Phys. Lett.* **99** 242501